

Molecular Dynamics Simulation of Liquid Gallium Electrospray Thrusters

IEPC-2009-181

*Presented at the 31st International Electric Propulsion Conference,
University of Michigan • Ann Arbor, Michigan • USA
September 20 – 24, 2009*

DaeYong Kim¹ and Michael M. Micci²

Department of Aerospace Engineering, The Pennsylvania State University, University Park, PA, 16802, USA

Molecular Dynamics (MD) is used to simulate the emission of gallium ions and ion clusters from a liquid gallium filled platinum capillary by an electric field generated by an extraction ring at a negative potential. MD solves the equations of motion in three dimensions for each gallium ion subject to interatomic and electrostatic forces. Liquid gallium properties such as viscosity, surface tension and wetting of the platinum capillary wall are results of the MD simulations and are not required a priori. Interactions between gallium atoms and wall platinum atoms are modeled using Lennard-Jones 12-6 potentials. The platinum capillary wall is modeled by multi-layers of platinum atoms located at fixed metal lattice sites. Maxwell's Equations are simultaneously solved for the electric field between the capillary and the downstream extraction ring with and without the presence of space charge. Simulations show the formation of the liquid gallium Taylor cone and the extraction and acceleration of gallium ions and ion clusters. Simulation results include current and ion velocity. The effects of extraction voltage, extraction electrode inner radius and separation distance between the capillary and extraction electrode are shown via the simulation.

Nomenclature

E_x	=	x component of electric field
E_y	=	y component of electric field
E_z	=	z component of electric field
Q	=	space charge
q	=	electron charge
r_c	=	cutoff radius
r_{ij}	=	distance between gallium atom i and atom j
U	=	Lennard-Jones potential
V_o	=	voltage on capillary
V_f	=	voltage on extraction ring
$\epsilon_{gg}, \epsilon_{pp}$	=	Lennard-Jones energy parameters for gallium and platinum
σ_{gg}, σ_{pp}	=	Lennard-Jones distance parameters for gallium and platinum
ϕ	=	electric potential

¹ Graduate Student, Aerospace Engineering, duk162@psu.edu.

² Professor, Aerospace Engineering, micci@psu.edu.

I. Introduction

The first electro spray using liquid metal droplets as a propellant was developed by Krohn for application in space propulsion in the 1960s¹. In the last few years electro spray propulsion systems have been of increasing interest because of satellite missions requiring micro- and nano-satellites to operate in the form of a constellation. For these missions it is necessary to operate with high precision a propulsion system capable of maneuvering a satellite's

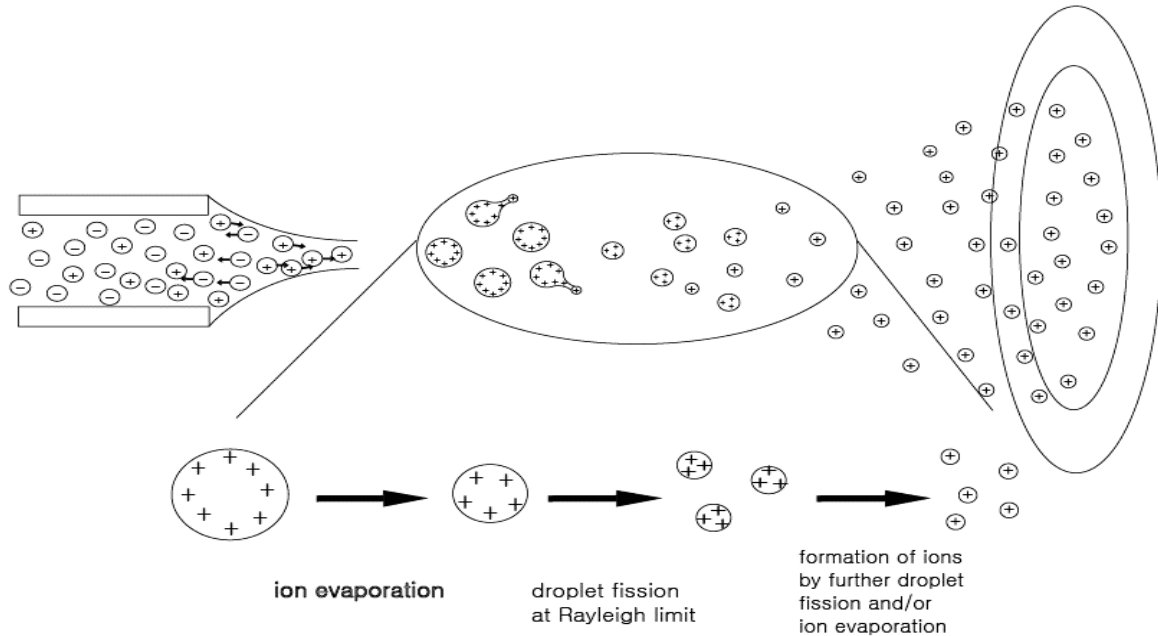


Figure 1. Schematic presentation of droplets production in electro spray and the formation of the Taylor cone. Liquid gallium is formed in the Taylor cone at the tip of platinum capillary and the emitted droplets of gallium disintegrate into the smaller droplets by the ion evaporation and the Rayleigh limit. Gallium ions and ions clusters created by this process are extracted by an electric field generated by an extraction ring at a negative potential.

positions within a few nanometers.

Before a high negative voltage is imposed between two electrodes, capillary and extraction ring, a liquid has the same amount of its positive and negative charges. There are no external forces acting on the liquid, herein an electrical force is induced by electric field. Therefore the surface tension works in such a way to minimize the surface of the liquid. When a high negative voltage is applied on the extraction ring and the capillary which plays a role as the ground electrode, some positive ions in the liquid move toward the surface of liquid and some negative ions move backward until the imposed field inside the liquid is eliminated by the redistribution of charges. Positive ions near the liquid surface give rise to a destabilized liquid surface, because they are drawn by the shear stress that is generated by the electric force on the liquid surface but cannot come out of it. This shear stress elongates the liquid meniscus to form a cone called the Taylor cone. The electric field beyond a certain critical value causes the loss of stability, and then makes a liquid issue from a capillary in the form of a jet. The jet emits along the capillary axis or deflects from it only on an angle less than 10° . At some distance downstream this liquid jet becomes unstable and breaks up into small charged droplets via a “budding” process when the surface tension is exceeded by the electric force as shown Figure 1². The diameter of the droplets is affected by the various parameters such as the applied voltage, liquid properties, and so on³. Charged droplets produced from the tip of the Taylor cone shrink by ion evaporation until they reach the Rayleigh limit⁴. At the Raleigh limit the magnitude of droplet charge is sufficient to overcome the surface tension, leading to the disintegration of the droplet. The droplets are not split evenly into two smaller droplets having approximately equal mass and charge. This repeated process ultimately leads to very small, highly charged droplets. In general the charged droplets undergo an oscillation to cause disruptions in which the parent droplets emit a tail of much smaller sibling droplets⁵. The emitted sibling droplets have around 2% of the mass of the parent droplets, while their charge is about 15% of the parent droplets⁶.

II. Model of Liquid Gallium

MD (molecular dynamics) simulations were carried out with constant density and constant volume in a cubic box. We applied periodic boundary conditions in the x, y, and z directions and employed the velocity Verlet algorithm to integrate the motion of atoms with respect to time. Unlike a general cut-off distance that is 2.5 times the sigma value in the Lennard-Jones 12-6 potential, the force cut-off distance was fixed at 10.5 Å. The number of gallium atoms was 87,808 ($28 \times 28 \times 28 \times 4$) and the sides of the box were 1.1984×10^{-8} m ($28 \times 4.28 \times 10^{-10}$ m). A large cubic box in which all of gallium atoms are included is the configuration of many tiny cells. A tiny cell has four atoms of gallium. The Figure 2 shows a cubic box and a cell.

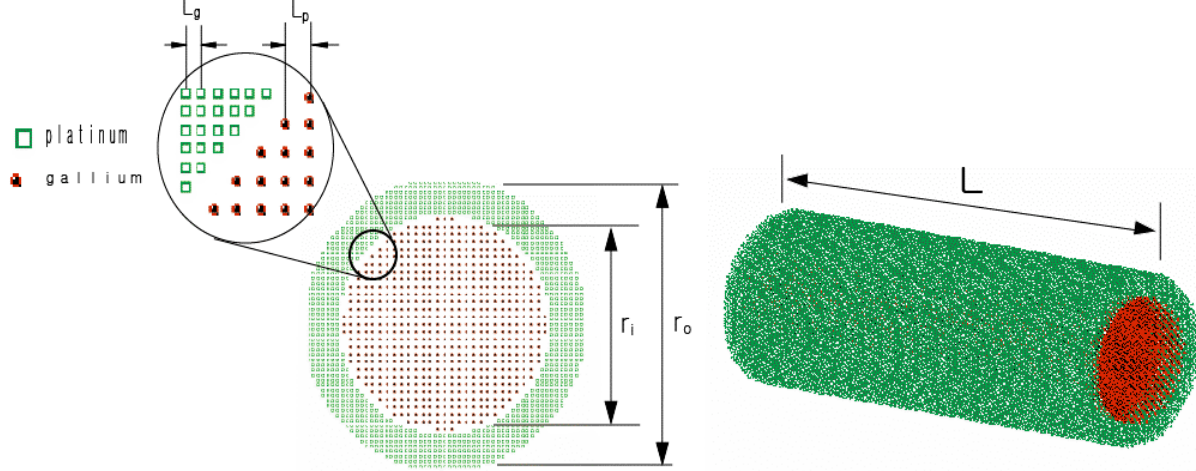


Figure 2. The initial setup of gallium atoms in platinum capillary. Gallium and platinum atoms are arranged in an fcc structure. L_p and L_g are the lattice spacing of gallium atom and platinum atoms, respectively. The lattice spacing of gallium atoms was determined so that the density of gallium in a capillary was equal to the mass density at 320K. The lattice spacing of platinum atom was fixed at 2.77×10^{-10} m.

The length of the lattice spacing was estimated so that the density of gallium in a cubic box was equal to the mass density ($\rho = 5.904 \text{ g/cm}^3$) above the melting temperature. The platinum capillary was represented by a layer of fcc with the lattice spacing of 2.77×10^{-10} m⁷. The length of a capillary (L) was 10 nm, the inner radius of capillary was 3 nm, and the outer radius was 4 nm. All the atoms have initial velocities which are determined by the Maxwell-Boltzmann distribution at a given temperature. We considered only the attribution of short-range forces to the motion of gallium atoms and used the link-list method to be more effective in calculation time⁸. Atoms of gallium have two kinds of potential energy. One is the potential energy interacting with each atom of gallium. The other is the potential energy interaction between gallium atoms and platinum atoms. There is no potential energy between platinum atoms because they are fixed. The potential functions of gallium-gallium and gallium-platinum were approximately described with a Lennard-Jones 12-6 potential. The interactions of atoms are truncated and shifted with a cutoff distance r_c :

$$U^{LJ}(r_{ij}) = \begin{cases} U^{LJ}(r_{ij}) - U^{LJ}(r_c) & r_{ij} < r_c \\ 0 & r_{ij} > r_c \end{cases} \quad (1)$$

with

$$U^{LJ} = 4\epsilon_{ij} \left[\left(\frac{\sigma}{r_{ij}} \right)^{12} + \left(\frac{\sigma}{r_{ij}} \right)^6 \right]$$

where r_{ij} is the distance between atoms i and j , σ is the distance to the zero in $U^{LJ}(r_{ij})$ and ϵ is the energy at the minimum in $U^{LJ}(r_{ij})$. To obtain two parameters in the potential function for two different kinds of atoms, gallium and platinum, we adopted the Lorentz-Berthelot rule shown in Equation 2.

$$\begin{aligned}\sigma_{gp} &= \frac{1}{2} [\sigma_{gg} + \sigma_{pp}] \\ \varepsilon_{gp} &= \sqrt{[\sigma_{gg}\sigma_{pp}]}\end{aligned}\quad (2)$$

We also can obtain the forces acting on an atom by other atoms with the pair potential presented above. Provided a pair of atoms i and j can be identified the squared intermolecular distance can be easily known by the minimum image separation. The force on atom i by j is

$$\begin{aligned}\vec{f} &= -\nabla U(r) \\ \vec{f} &= \frac{24\varepsilon}{r^2} \left[2 \left(\frac{\sigma}{r_{ij}} \right)^{12} - \left(\frac{\sigma}{r_{ij}} \right)^6 \right] \vec{r}\end{aligned}\quad (3)$$

The force on atom j by atom i is obtained by employing Newton's third law. We ran the MD simulation over 15000 time steps with 2.5 fs interval in time and applied the rescaled velocity until the 7500th time step. The numerical scheme used to integrate the motion of gallium atoms was the velocity Verlet algorithm and the linked-list method was used to avoid expensive calculations. The periodic boundary condition was applied only in the longitudinal direction. The motion in radial direction was restricted by the potential between gallium and platinum.

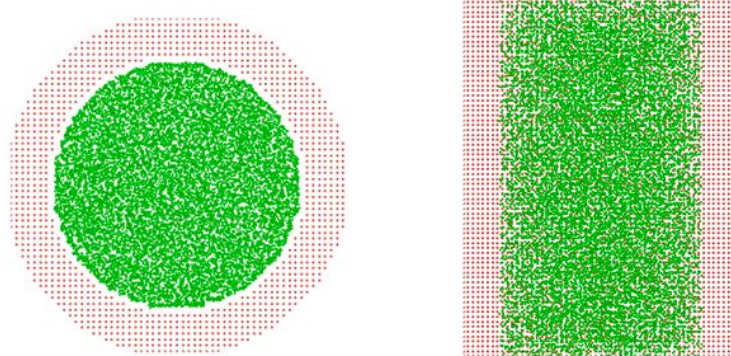


Figure 3. The gallium atoms in capillary at the equilibrium state. *The gallium atoms in the platinum capillary were rearranged after 15000 time steps with 2.5 fs time interval. The left figure shows the distribution of gallium atoms at equilibrium on a cross section, the right figure shows that on a side view.*

III. Electro spray Thruster Simulation

A. Electric Potential

Poisson's equation is solved to obtain the electric force acting on the gallium ions in an electric field. To this end it is needed to specify an initial condition as well as boundary condition. The configuration of the electro spray thruster created for simulation is shown Figure 4. The length and size of a capillary and an extraction ring used in the electro spray thruster simulation and the boundary condition applied to this simulation are represented in Table 1 and Table 2, respectively.

area	area	area	area	area	area	capillary	extraction
1234	5678	1256	3478	2375	1486		ring
0	0	0	0	0	0	V_0	V_f

Table 1. The gallium atoms in capillary at the equilibrium state. *The gallium atoms in platinum capillary were rearranged after 15000 time steps with 2.5fs time interval. The left figure shows the distribution of gallium atoms at equilibrium on a cross section, the right figure show that on a side view.*

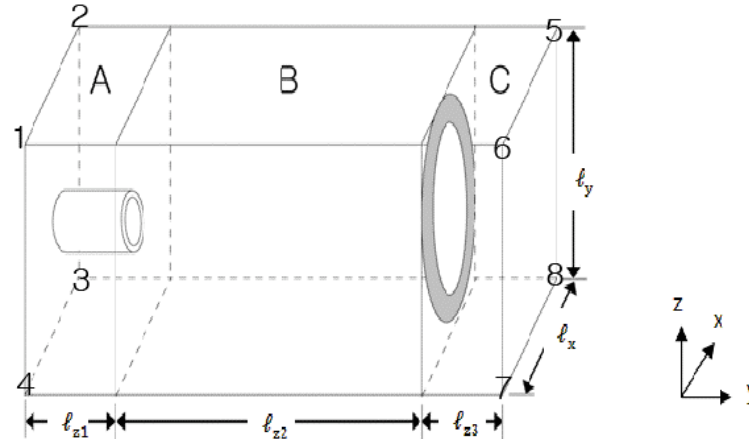


Figure 4. The domain for the calculation of the electric potential and the configuration of a capillary and an extraction ring. l_{z1} is the length of a capillary, and l_{z2} is the separation between two electrodes, a capillary and an extraction ring.

Before Poisson's equation, we first solved the Laplace equation in which the effect of space charge is not taken into account. Since a FEM has an advantage over a FDM in representing properties of field and Neumann boundaries, we used FEM (finite element method) rather than FDM (finite difference method) in this field problem. And rather than using an irregular mesh, we made the use of FEM on a regular mesh because in three dimensions an irregular mesh has to store much information on the position of the mesh. In addition it is not easy to generate an irregular mesh in three dimensions. Figure 5 shows the mesh parameters near a point of interest in the calculation of Poisson's equation. Each point has six neighbor vertices and these six vertices have their own potential ϕ_{xu} , ϕ_{xd} , ϕ_{yu} , ϕ_{yd} , ϕ_{zu} , and ϕ_{zd} . The distance to these neighboring vertices are h_{xu} , h_{xd} , h_{yu} , h_{yd} , h_{zu} , and h_{zd} . There are eight elements surrounding a test point and they have their own relative dielectric constant and space charge density denoted by the symbol, for example, ϵ_{udu} , ρ_{uuu} . Under the assumption that the space between a capillary and an extraction electrode is a vacuum, the relative dielectric constant of the media is 1. Here the index order, i , j , and k refer to the x , y , and z directions, respectively. Taking a Gaussian surface integral over a box extending parallel to the axes halfway to each neighbor, the space charge at a test point is found⁹. In our simulation h_{xu} , h_{xd} , h_{yu} , and h_{yd} have the same value of 1.0×10^{-9} m in all regions A, B and C, whereas h_{zu} and h_{zd} have different lengths in these regions. The values of h_{zu} and h_{zd} in region A are 1.0×10^{-9} m and those in regions B and C are 5.0×10^{-9} m.

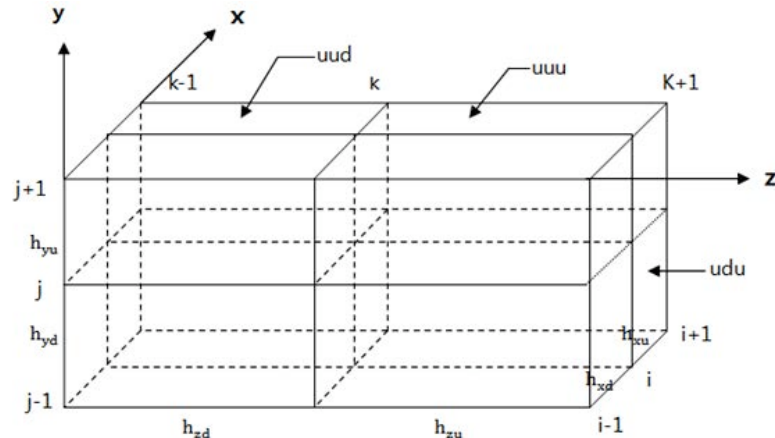


Figure 5. Mesh convention and Gaussian volume near a test point for a three-dimensional finite-element electrostatic solution⁹. h_{xu} , h_{xd} , h_{yu} , h_{yd} , h_{zu} , and h_{zd} are the distances to the neighboring vertices.

$$\phi_{i,j,k} = \frac{W_{xu}\phi_{xu} + W_{xd}\phi_{xd} + W_{yu}\phi_{yu} + W_{yd}\phi_{yd} + W_{zu}\phi_{zu} + W_{zd}\phi_{zd} + Q_{i,j,k}}{W_{xu} + W_{xd} + W_{du} + W_{yd} + W_{zu} + W_{zd}} \quad (4)$$

$$Q_{i,j,kz} = \frac{1}{8\epsilon_0} \left[h_{xu}h_{yu}h_{zu}\rho_{uuu} + h_{xd}h_{yu}h_{zu}\rho_{duu} + h_{xu}h_{yd}h_{zu}\rho_{udu} + h_{xd}h_{yd}h_{zu}\rho_{ddu} \right. \\ \left. + h_{xu}h_{yu}h_{zd}\rho_{uud} + h_{xd}h_{yu}h_{zd}\rho_{dud} + h_{xu}h_{yd}h_{zd}\rho_{udd} + h_{xd}h_{yd}h_{zd}\rho_{ddd} \right] \quad (5)$$

$$W_{xu} = \frac{1}{4h_{xu}} [h_{yu}h_{zu} + h_{yd}h_{zu} + h_{yu}h_{zd} + h_{yd}h_{zd}]$$

$$W_{xd} = \frac{1}{4h_{xd}} [h_{yu}h_{zu} + h_{yd}h_{zu} + h_{yu}h_{zd} + h_{yd}h_{zd}]$$

$$W_{yu} = \frac{1}{4h_{yu}} [h_{xu}h_{zu} + h_{xd}h_{zu} + h_{xu}h_{zd} + h_{xd}h_{zd}]$$

$$W_{yd} = \frac{1}{4h_{yd}} [h_{xu}h_{zu} + h_{xd}h_{zu} + h_{xu}h_{zd} + h_{xd}h_{zd}]$$

$$W_{zu} = \frac{1}{4h_{zu}} [h_{xu}h_{yu} + h_{xd}h_{yu} + h_{xu}h_{yd} + h_{xd}h_{yd}]$$

$$W_{zd} = \frac{1}{4h_{zd}} [h_{xu}h_{yu} + h_{xd}h_{yu} + h_{xu}h_{yd} + h_{xd}h_{yd}] \quad (6)$$

B. Space Charge

In addition to the estimated value of potential at all vertices, it is necessary to know that how many gallium ions each cell has for solving Poisson's equations completely. Cells generated to calculate the potential are used once again in the calculation of the space charge. In order to know which cell has how many gallium ions, the index number in sequence is assigned to each cell as Figure 6 shows.

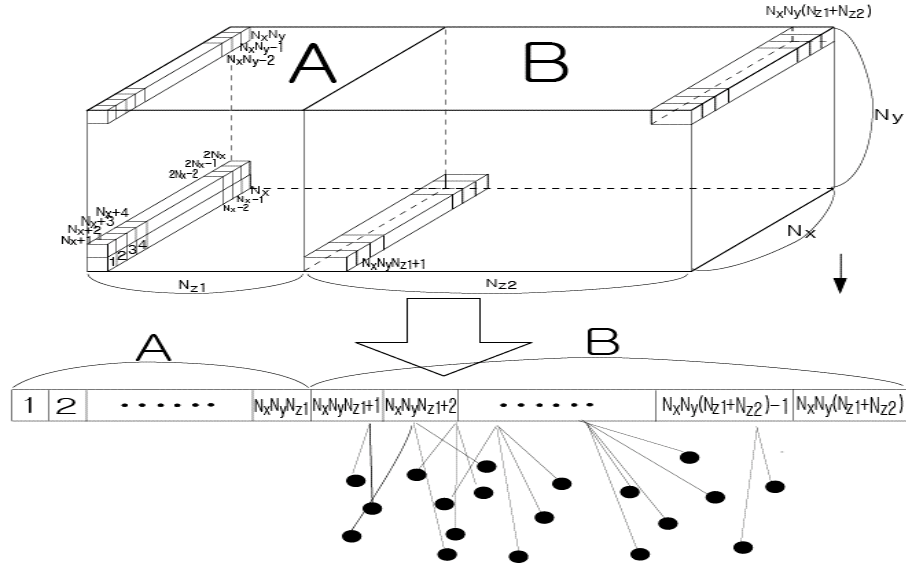


Figure 6. The assignment of gallium ions in region B into each cell. The domain of calculation for solving Poisson's equation was divided into $N_x \times N_y \times (N_{z1} + N_{z2})$ cells. Each cell has its own index number. Region A is within the length of the capillary. Therefore region A has no gallium ions.

The index number of the cell in which each ion lies can be given by Equation 7. Under the assumption that most of the gallium ions emitting from a capillary would move in the region from the capillary tip to an extraction ring we took account of the ions in the region.

$$\begin{aligned}
index = & 1 + \text{int} \left\{ \left[\left(r_{x(i)} + \frac{L_x}{2} \right) \times N_x \right] \times \frac{1}{N_x \times h_x} \right\} \\
& + \text{int} \left\{ \left[\left(r_{y(i)} + \frac{L_y}{2} \right) \times N_y \right] \times \frac{1}{N_y \times h_y} \right\} \times N_x \\
& + \text{int} \left\{ \left[\left(r_{z(i)} - L_{capillary} \right) \times N_{z2} \right] \times \frac{1}{N_{z2} \times h_{z2}} \right\} \times N_x \times N_y \\
& + N_{z1} \times N_x \times N_y
\end{aligned} \tag{7}$$

where L_x , L_y , and $L_{capillary}$ are the lengths of the domain in the x and y directions and the length of the capillary, and N_x , N_y and N_z are the number of cells in the x, y, and z directions, respectively. The symbol $\text{int}\{A\}$ denotes the closest integer number to the real number A. After sorting all gallium ions in each cell, we can easily calculate the space charge in Poisson's equation using $\rho_i = q \times \text{number of gallium ions in } i_{th} \text{ cell}$ where q is the electron charge ($q = 1.6022 \times 10^{-19} \text{ C}$).

C. Electric Field

An electric field at each vertex is given by the relationship (Equation 8) between an electric field and electric potential.

$$\vec{E} = -\nabla\phi \tag{8}$$

This above equation can be represented in the numerical form with second order accuracy using a finite difference method.

$$\begin{aligned}
\vec{E}_x &= - \left[\frac{\phi_{i+1,j,k} - \phi_{i-1,j,k}}{h_{xu} - h_{xd}} \right] \\
\vec{E}_y &= - \left[\frac{\phi_{i,j+1,k} - \phi_{i,j-1,k}}{h_{yu} - h_{yd}} \right] \\
\vec{E}_z &= - \left[\frac{\phi_{i,j,k+1} - \phi_{i,j,k-1}}{h_{zu} - h_{zd}} \right]
\end{aligned} \tag{9}$$

The value of the electric force acting on an ion of gallium in a cell can be found by interpolation. The gallium ion is at the position of r_x , r_y and r_z in the rectangular coordinates, respectively. There is no electric field on the platinum capillary and ions of gallium in the platinum capillary since we made the assumption that both gallium and platinum are perfectly conducting materials.

IV. Numerical Results

To characterize the effect of several variables of the electrospray, we varied the distance between a capillary and an extraction ring (L), the operating voltage (V_f), and the inner radius of the extraction ring (r_i). All of the three cases used the same capillary whose inner and outer radii were $3 \times 10^{-9} \text{ m}$ and $4 \times 10^{-9} \text{ m}$, respectively. The outer radius of the extraction ring remained as $80 \times 10^{-9} \text{ m}$.

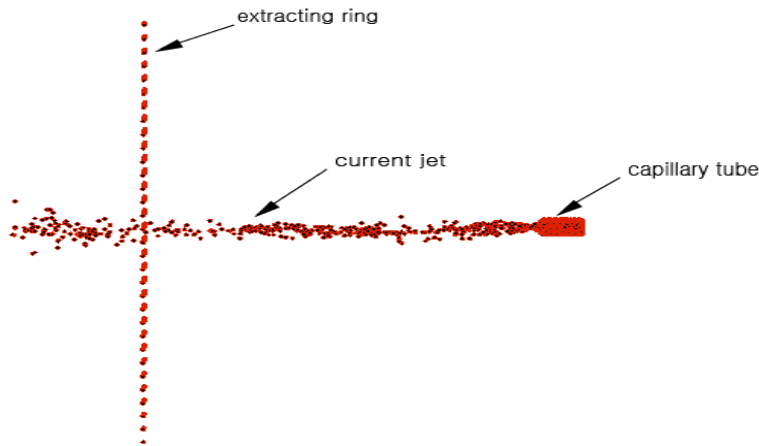


Figure 7. The configuration of electro spray and the Taylor cone in simulation. The simulation of electro spray thruster was created at the operating voltage of -700 V for 4.0×10^{-11} seconds. The distance between two electrodes was $1.0 \times 10^{-7}\text{ m}$, and the inner and outer radii of extraction ring were $3.0 \times 10^{-9}\text{ m}$ and $80.0 \times 10^{-9}\text{ m}$, respectively. The inner and outer radii of the capillary were $3.0 \times 10^{-9}\text{ m}$ and $4.0 \times 10^{-9}\text{ m}$.

A. Electrode distance effect

The simulation was conducted over 15000 time steps with 2.5 fs interval in time with conditions that the constant operating voltage was -700 V , and the inner radius of the extraction ring was $3 \times 10^{-9}\text{ m}$. We increased the distance between the two electrodes, the extraction ring and the tip of the capillary, by $0.1 \times 10^{-7}\text{ m}$ from $0.7 \times 10^{-7}\text{ m}$ to $1.2 \times 10^{-7}\text{ m}$. The plots of the total current and the average velocity versus the distance are presented in Figure 8. As seen in this figure the total current dropped sharply at a distance of $2.2 \times 10^{-7}\text{ m}$. This is because at this distance a current beam losses stability, and decreases the total number of gallium ions passing through the extraction ring. That leads to the decrease in total current. As the extraction ring is positioned further away the instability becomes stronger and the total current increasingly goes down. The average velocity in the z direction decreased as the separation between the two electrodes increased. In contrast to that the total current dropped steeply at the distance of $2.2 \times 10^{-7}\text{ m}$, the average velocity went down gradually. This is because the extraction force on gallium ions was not affected by the instability of the current beam but by the electric field, that is, the separation between the two electrodes.

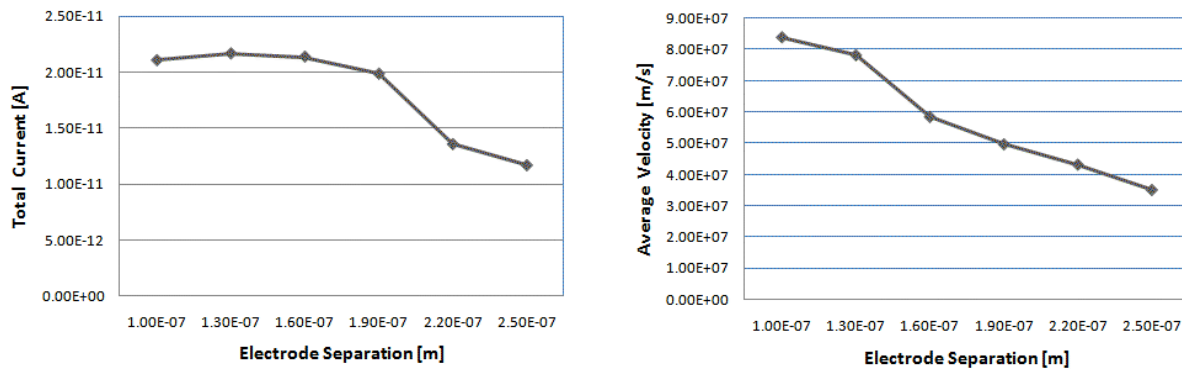


Figure 8. The effect of electrode separation on ion current and velocity. The simulation of the electro spray thruster was created at the operation voltage of -700 V for 4.0×10^{-11} seconds. The distance between the two electrodes was $1.0 \times 10^{-7}\text{ m}$, and the inner and outer radii of the extraction ring were $3.0 \times 10^{-9}\text{ m}$ and $80.0 \times 10^{-9}\text{ m}$, respectively. The inner and outer radii of the capillary were $3.0 \times 10^{-9}\text{ m}$ and $4.0 \times 10^{-9}\text{ m}$.

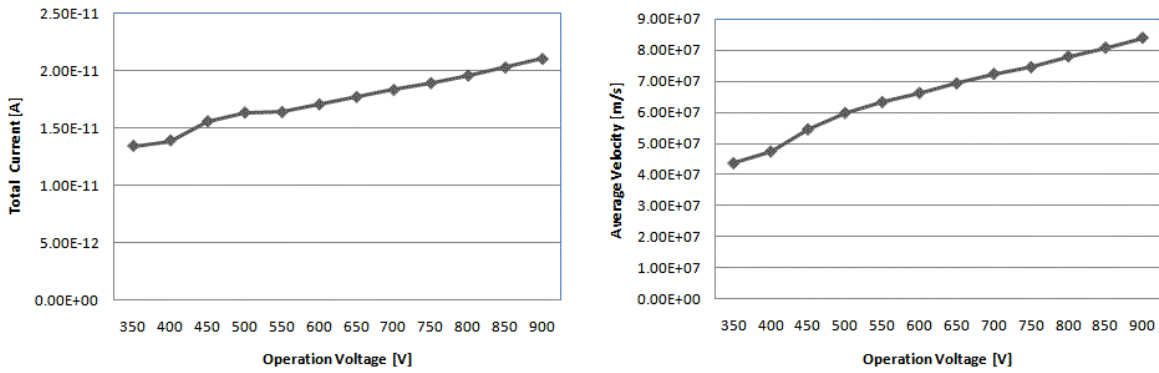


Figure 9. The effect of operating voltage on ion current and velocity. The simulation of the electrospray thruster was created at the operation voltage of -700 V for 4.0×10^{-11} seconds. The distance between two electrodes was 1.0×10^{-7} m, and the inner and outer radii of extraction ring were 3.0×10^{-9} m and 80.0×10^{-9} m, respectively. The inner and outer radii of capillary were 3.0×10^{-9} m and 4.0×10^{-9} m.

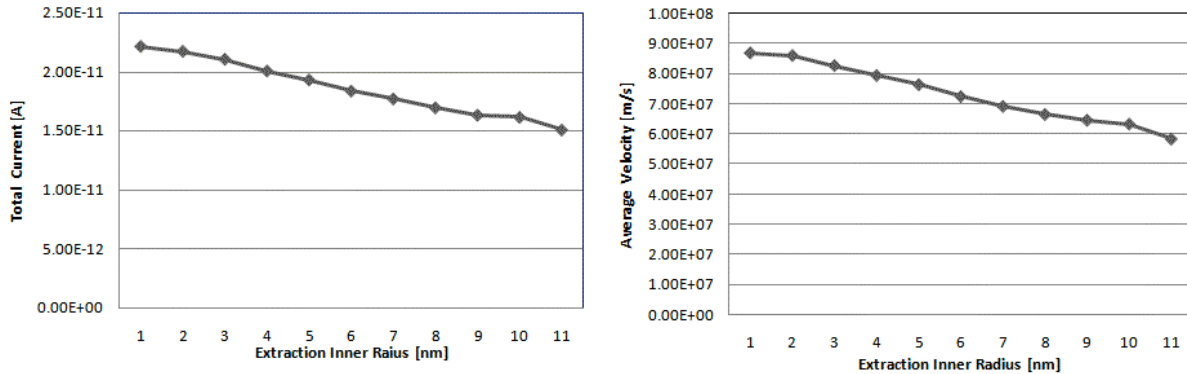


Figure 10. The effect of extraction electrode inner radius on ion current and velocity. The simulation of the electrospray thruster was created at the operation voltage of -700 V for 4.0×10^{-11} seconds. The distance between two electrodes was 1.0×10^{-7} m, and the inner and outer radii of the extraction ring were 3.0×10^{-9} m and 80.0×10^{-9} m, respectively. The inner and outer radii of the capillary were 3.0×10^{-9} m and 4.0×10^{-9} m.

B. Operation Voltage Effect

We carried out the simulation over 15000 time steps with 2.5 fs interval in time with both the capillary tube and the extraction ring at a fixed separation of 1×10^{-7} m, varying the operating voltage by -50 V from -350 V to -900 V. The inner and outer radii of the extraction ring were 3×10^{-9} m and 80×10^{-9} m, respectively. The dependence of the total current and the average velocity on the operating voltage is shown in Figure 9. This plot shows that the total current of the electrospray has an approximately linear dependence on the operating voltage. Since the electric force induced by an electric field is $F_e = q \times E$ the higher voltage, that is, the higher intensity of electric field generates the stronger attractive force on ions of gallium toward the extraction ring. The average velocity in z direction rose gradually as the operating voltage became higher because the higher voltage generated the stronger force on gallium ions toward the extraction ring.

C. Inner Radius of Extraction Ring Effect

The simulation was conducted over 15000 time steps with 2.5 fs interval in time with the same capillary tube as before. The reference operating voltage was -700 V, the separation was 1.0×10^{-7} m, and the outer radius of the extraction ring was 80×10^{-9} m. The inner radius was increased by 1.0×10^{-9} m from 6×10^{-7} m to 11×10^{-7} m. The inner and outer radii of the extraction ring have an influence on the divergence angle of emitted gallium ions. In

particular, the stability as well as the divergence of the jet has a considerable dependence on the inner radius rather than the outer radius because the ions of gallium passing through the extraction ring make a contribution to the variation of the electric potential and electric field around the inner radius. Figure 10 represents the effect of the inner radius of the extraction ring on the total current and the average velocity. The result shows that the total current has a linear dependence on the inner radius of the extraction ring. This is because the extraction ring with the smaller inner radius made a more convergent current beam, which generated the higher total current. Also the smaller inner radius of the extraction ring focused a stronger component of the electric potential into the acceleration force in the z direction on the gallium ions. That allowed the gallium ions to have a faster average velocity.

V. Conclusions

This work was carried out to analyze the characteristics of electrosprays numerically on the microscopic scale using molecular dynamics simulations rather than using fluid equations such as the Navier-Stokes equations used on the macroscopic scale. Of the many variables that affect the features of electrosprays, we varied the separation between the extraction ring and a capillary, the applied voltage on the two electrodes, extraction ring and capillary, and the inner radius of the extraction ring. First, a farther distance between the two electrodes caused the total current as well as the number of particles passing through the extraction ring to decrease since the increase in the distance between the two electrodes with constant voltage caused a decrease in the electric field. Beyond a certain distance the emitted jet came to be unstable, which led to the sharp drop in both the total current and the number of particles. Secondly, the higher operating voltage, that is, the higher electric field at fixed separation means that there is stronger attractive force on ions of gallium between the two electrodes. Therefore the higher voltage allowed more ions of gallium to pass the extraction ring, which created the higher total current. Finally, since the extraction ring serves to attract the charged particles of gallium liquid, the size of the extraction ring, especially the inner radius had an influence on the stability and the shape of the jet. The smaller radius made a more convergent jet and allowed ions of gallium to have a higher velocity in the z direction. That served to make a jet with a higher current with the extraction ring with a smaller inner radius.

Acknowledgments

The authors thank Abraham Mathew and Kirk Heller for their technical support with computers used for this simulation.

References

- ¹ Krohn, V. E., "Liquid Metal Droplets for Heavy Particle Propulsion," ARS Electrostatic Propulsion Conference, Monterey, CA, 3-4, 1960.
- ² Kebarle, P. and Tang, L., "From Ions in Solution to Ions in the Gas Phase," Anal. Chem. 65, 22 (1993).
- ³ Wilm, M. S. and Mann, M., Int. J. Mass Spectrom, "Electrospray and Taylor Cone theory, Dole's beam of macromolecules at last?", Int. J. Mass Spectrom. Ion processes 136, 167 (1994).
- ⁴ Lord Rayleigh, Phil. Mag. 14, 184 (1882)
- ⁵ Achtzehn, T., Muller, R. and Duft, D., "The Coulomb Instability of Charged Microdroplets: Dynamics and Scaling", Eur. Phys. J. D. 34. 311-313 (2005)
- ⁶ Gomez, A. and Tang, K., "Charge and Fission of Droplets in Electrostatic Sprays", Phys. Fluid 6. 404 (1994)
- ⁷ Shalabh C., Marro, J. and Chun, N., "Molecular Dynamic Simulation of Platinum Heater and Associated Nano-scale Liquid Argon Film Evaporation and Colloidal Adsorption Characteristics", J. Colloid interface sci., 328, 134-146 (2008)
- ⁸ Peyret, R., and Taylor, T. D., *Computational Methods in Fluid Flow*, 2nd ed., Springer-Verlag, New York, 1983, Chaps. 7, 14.
- ⁹ Humpries, S. Jr., *Field Solutions on Computer*, 1st ed., CRC Press, 1998, Chaps. 4, 6.